

1 Double Mammary In Situ: Predicting Feasibility of Right Mammary Artery In Situ for  
2 Circumflex Coronary Artery System

3 Rafik Margaryan, MD, PhD<sup>1,2</sup>, Daniele Della Latta<sup>2</sup>, Giacomo Bianchi, MD, PhD<sup>1</sup>, Nicola  
4 Martini<sup>2</sup>, Andrea Gori<sup>2</sup>, & Marco Solinas<sup>1</sup>

5 <sup>1</sup> Adult Cardiac Surgery, Ospedale Del Cuore, Fondazione G Monasterio

6 <sup>2</sup> Deep Learning Unit, Ospedale Del Cuore, Fondazione G Monasterio

7 Author Note

8 Correspondence concerning this article should be addressed to Rafik Margaryan, MD,  
9 PhD, Via Aurelia Sud 303. E-mail: [margaryan@ftgm.it](mailto:margaryan@ftgm.it)

10

## Abstract

11 Objectives: Double (bilateral) mammary artery in situ revascularization seems less  
12 attractive to surgeons because of limited mammary length of right mammary artery, scare,  
13 or no means of its length estimation. Methods: We've selected patients who have used  
14 bilateral mammary artery for revascularization and divided them into two groups: in situ  
15 and y-graft groups. We have used preoperative chest x-rays to build a predictive model with  
16 neural networks that could predict feasibility of in situ bilateral mammary revascularization.  
17 Results: The predictive model was able to predict a positive outcome with 96% percent  
18 accuracy ( $p < 0.01$ ). Models sensitivity and specificity were 96% and 95% respectively.  
19 Neural networks can be used to predict double mammary feasibility using chest x-rays.  
20 Model is capable of predicting positive outcomes with 95% accuracy. Conclusions: Chest  
21 x-ray base model can accurately predict the feasibility of in situ bilateral mammary artery  
22 revascularization.

23 *Keywords:* coronary artery disease, myocardial revascularization, neural networks,  
24 artificial intelligence

25 Word count: 1099

26 Double Mammary In Situ: Predicting Feasibility of Right Mammary Artery In Situ for  
27 Circumflex Coronary Artery System

28 **Introduction**

29 The use of double (bilateral) internal mammary arteries (BIMA) is scarcely diffused in  
30 the real world (ElBardissi et al., 2012; LaPar et al., 2015), despite being supported by robust  
31 evidence over the last two decades. Right internal mammary artery (RIMA) is anatomically,  
32 histologically and functionally similar to left mammary artery (LIMA), also in terms of  
33 endothelial function and RNA expression level (Ferrari et al., 2014; Märkl, Raab, Arnholdt,  
34 & Vicol, 2003).

35 Lack of standardization for the appropriate use of the right internal mammary artery  
36 (RIMA) has limited its routine use in myocardial revascularization. RIMA can be  
37 anastomosed in situ to the left anterior descending artery (LAD) or to the proximal branches  
38 of the circumflex artery, but its length may pose technical challenges. Although  
39 skeletonization is a technique that provides better internal mammary artery (IMA) length, it  
40 is not widely accepted. As a result, it is not always possible to choose the best anastomotic  
41 site, and we are forced to graft the RIMA according to its length rather than the most  
42 suitable coronary artery segment. Alternatively, the RIMA can be used as a free graft, which  
43 is anastomosed to the left internal mammary artery (LIMA) as a composite conduit. This  
44 option is more technically demanding and can expose to higher rates of competitive flow  
45 with increased graft failure (Pevni et al., 2007) though no definitive data are available to  
46 confirm this finding (Glineur et al., 2008). Mid-term clinical outcome seems to be similar  
47 regardless of BIMA configuration, either in situ or as a composite conduit (Glineur et al.,  
48 2008). In situ double mammary grafting is safe and durable bypass strategy when  
49 circumference artery system has suitable targets, although personal judgment of right  
50 mammary length, hence, RIMA in situ feasibility remains subjective.

51 We sought to develop a prediction model using chest x-ray and deep neural networks in  
52 order to estimate the feasibility of right mammary artery to circumflex artery targets (early  
53 obtuse marginal branches and intermediate/early diagonal arteries)

## 54 **Material and Methods**

### 55 **Patients**

56 We have selected patients from our electronic health record system, undergoing double  
57 mammary artery grafting from 2007 until August 2019 ( $n = 292$ ) were selected for this study.  
58 All patients underwent successful on-pump bypass surgery. For this analysis we've ignored  
59 other types of bypasses. We divided the population into two groups:

- 60 • In situ bypass grafting
- 61 • Grafting using y- or t-grafts

62 127 were double mammary grafts in-situ and 165 were double mammary grafts Y  
63 grafts. Mean age of the patients was  $61.4 \pm 7.7$ . All other demographic data are presented  
64 in Table 1. All patients had preoperative chest x-ray (antero-posterior and lateral).

### 65 **Data Acquisition and Processing**

66 292 chest digital X-ray examinations (DX) were performed on patients enrolled for  
67 valvular surgery. X-ray images of lateral latero (LL) projections were used to train a deep  
68 convolutional neural network (DNN). All DX were taken with standing patient placed 180  
69 cm from the X-ray tube using a digital flat detector panel with a spatial resolution of  
70  $0.139 \times 0.139$  mm<sup>2</sup>. The size of the image matrix is variable (2500x2500-4000x4000 px)  
71 depending on the size of the patient's chest as well as the X-ray exposure. The potential  
72 difference (kV) and exposure current (mAs) parameters are set automatically of the X-ray

73 scanner in order to obtain an adequate contrast independently of the variation of the  
74 attenuation of the body of each patient. The dataset was splitted into 183 images to train  
75 the DNN and 22 to test the learning. The size of all the images was readjusted to 2000x2000  
76 with a centered crop operation so as to maintain the DNN input layer with fixed size and  
77 partially mask the background that does not provide an useful information for the  
78 classification task. Finally, to minimize the computational load for network training, the  
79 images were scaled to 512x512 px. Whole data was divided randomly into two parts: train  
80 dataset and test dataset. Train dataset was used to create the model and validate it. Test  
81 dataset was used for only external validation and never has been used for tuning or  
82 improving the algorithm.

### 83 **Network Architecture**

84 A GoogLeNet network (Szegedy et al., 2014) was used to perform the classification task.  
85 The outline of the proposed architecture was reported in Table 1. The network comprises 22  
86 trainable layers and is made by nine Inception module stacked upon each other. A single  
87 Inception module represents a combination of 1x1, 3x3 and 5x5 convolutional kernels, used  
88 in parallel with the aim to progressively cover a bigger area and extract details (1x1) as more  
89 general features (5x5). The results are then concatenated with the outcome of a max-pooling  
90 layer and passed to the next layer. The presence of 1x1 convolutions before the 3x3, 5x5  
91 convolutions and after the pooling layer help to reduce the number of parameters in the  
92 Inception module and add more non-linearities to the network. To apply the GoogLeNet  
93 network architecture to the surgical task some implementation changes had to be made: 1)  
94 the input layer dimensions, set at 512 x 512, with a number of channels equals to one instead  
95 of three, being the inputs grayscale images; 2) in the output layer only two units were used,  
96 as we had to classify the images according the two possible locations of surgical incision; The  
97 network was designed and trained with TensorFlow (Workshop on Wireless Traffic

98 Measurements and Modeling, USENIX Association, ACM SIGMOBILE, ACM Special  
99 Interest Group in Operating Systems, & ACM Digital Library, 2016), running for 500 epochs  
100 on a single NVIDIA Titan Xp. Stochastic gradient descent and Adam optimizer were used to  
101 minimize a categorical cross-entropy for the network parameters update.

102 Schematic representation of the GoogLeNet network used to classify the input images.  
103 For a detailed description of the network architecture see (Szegedy et al., 2014).

104 The size of all the images was readjusted to 2000x2000 with a centered crop operation  
105 so as to maintain the DNN input layer with fixed size and partially mask the background  
106 that does not provide an useful information for the classification task. Finally, to minimize  
107 the computational load for network training, the images were scaled to 512x512 px. To  
108 evaluate the progress of learning the accuracy was calculated between the predicted and the  
109 real “point of incision.”

110

## Results

111 There were no hospital or 30 days mortality. In original model antero-posterior and  
112 lateral chest x-rays were include. However, lateral images were not changing or changing  
113 little of predictive value. The final model has only antero-posterior chest x-rays. Model has  
114 predicted with 95.55% accuracy ( $p < 0.01$ ). There were no significant differences in  
115 comorbidities divided by type of graft and sex group(see Table 1. Model’s sensitivity and  
116 specificity were 0.96 and 0.95. Area under curve (AUC) was 0.96. Predicted type and real  
117 type of configuration is reported in the Table 2. All combinations of grafts and type of  
118 revascularization see Table 3.

## Discussion

119

120 In this study we were able to build a predictive model using chest x-rays which does  
121 not require any type of measurement other than raw chest x-ray data with very high  
122 performs. To our knowledge it is first of its kind and it seeks to resolve an actual clinical  
123 problem. Absolute length of the bilateral mammary arteries is an intrinsic feature, and as we  
124 have demonstrated can be extracted if necessary. Hence, using medical imaging data is most  
125 accurate way to estimate intrinsic length of mammary arteries. Deep Learning models in  
126 general have very high good performance, and in this clinical scenario it has very high  
127 accuracy and AUC values for predicting possible double mammary in-situ bypass grafting. It  
128 proves to have hit sensitivity and specificity. It is particularly valuable for total arterial  
129 revascularization. Certainly it is bias by its nature of being single center. Future  
130 commitment for international chest x-ray database should be created for better model.  
131 Bilateral independent mammary arteries is most efficient and durable solution as state of the  
132 art in complete atrial revascularization(Head, Milojevic, Taggart, & Puskas, 2017). There  
133 are reports in literature that configuration does not change the mortality (Di Mauro et al.,  
134 2016). In any case when one does not want to comprise the left mammary artery and/or has  
135 a doubt on flows and distal resistances, the independent in situ configuration is the right  
136 choice to our experience and knowledge.

## Conclusion

137

138 Neural networks can be used to predict double mammary feasibility using chest x-rays.  
139 Model is capable of predicting positive outcome with 95.55% accuracy. It is unique, non  
140 operator dependent method which can be very valuable in clinical situations.

141

## Tables

142

## Figures



References

143

144 Di Mauro, M., Iacò, A. L., Allam, A., Awadi, M. O., Osman, A. A., Clemente, D., &  
145 Calafiore, A. M. (2016). Bilateral internal mammary artery grafting: In situ  
146 versus Y-graft. Similar 20-year outcome †. *European Journal of Cardio-Thoracic*  
147 *Surgery*, 50(4), 729–734. <https://doi.org/10.1093/ejcts/ezw100>

148 ElBardissi, A. W., Aranki, S. F., Sheng, S., O'Brien, S. M., Greenberg, C. C., &  
149 Gammie, J. S. (2012). Trends in isolated coronary artery bypass grafting: An  
150 analysis of the Society of Thoracic Surgeons adult cardiac surgery database. *The*  
151 *Journal of Thoracic and Cardiovascular Surgery*, 143(2), 273–281.  
152 <https://doi.org/10.1016/j.jtcvs.2011.10.029>

153 Ferrari, G., Quackenbush, J., Strobeck, J., Hu, L., Johnson, C. K., Mak, A., . . .  
154 Grau, J. B. (2014). Comparative genome-wide transcriptional analysis of human  
155 left and right internal mammary arteries. *Genomics*, 104(1), 36–44.  
156 <https://doi.org/10.1016/j.ygeno.2014.04.005>

157 Glineur, D., Hanet, C., Poncelet, A., D'hoore, W., Funken, J.-C., Rubay, J., . . . El  
158 Khoury, G. (2008). Comparison of bilateral internal thoracic artery  
159 revascularization using in situ or Y graft configurations: A prospective randomized  
160 clinical, functional, and angiographic midterm evaluation. *Circulation*, 118(14  
161 Suppl), S216–221. <https://doi.org/10.1161/CIRCULATIONAHA.107.751933>

162 Head, S. J., Milojevic, M., Taggart, D. P., & Puskas, J. D. (2017). Current Practice  
163 of State-of-the-Art Surgical Coronary Revascularization. *Circulation*, 136(14),  
164 1331–1345. <https://doi.org/10.1161/CIRCULATIONAHA.116.022572>

165 LaPar, D. J., Crosby, I. K., Rich, J. B., Quader, M. A., Speir, A. M., Kern, J. A., . . .  
166 Investigators for the Virginia Cardiac Surgery Quality Initiative. (2015). Bilateral

167 Internal Mammary Artery Use for Coronary Artery Bypass Grafting Remains  
168 Underutilized: A Propensity-Matched Multi-Institution Analysis. *The Annals of*  
169 *Thoracic Surgery*, 100(1), 8-14; discussion 14-15.  
170 <https://doi.org/10.1016/j.athoracsur.2015.02.088>

171 Märkl, B., Raab, S., Arnholdt, H., & Vicol, C. (2003). Morphological and  
172 histopathological comparison of left and right internal thoracic artery with  
173 implications on their use for coronary surgery. *Interactive Cardiovascular and*  
174 *Thoracic Surgery*, 2(1), 73–76. [https://doi.org/10.1016/S1569-9293\(02\)00102-0](https://doi.org/10.1016/S1569-9293(02)00102-0)

175 Pevni, D., Hertz, I., Medalion, B., Kramer, A., Paz, Y., Uretzky, G., & Mohr, R.  
176 (2007). Angiographic evidence for reduced graft patency due to competitive flow  
177 in composite arterial T-grafts. *The Journal of Thoracic and Cardiovascular*  
178 *Surgery*, 133(5), 1220–1225. <https://doi.org/10.1016/j.jtcvs.2006.07.060>

179 Szegedy, C., Liu, W., Jia, Y., Sermanet, P., Reed, S., Anguelov, D., . . . Rabinovich,  
180 A. (2014). Going Deeper with Convolutions. *arXiv:1409.4842 [Cs]*. Retrieved  
181 from <http://arxiv.org/abs/1409.4842>

182 Workshop on Wireless Traffic Measurements and Modeling, USENIX Association,  
183 ACM SIGMOBILE, ACM Special Interest Group in Operating Systems, & ACM  
184 Digital Library. (2016). *Papers presented at the Workshop on Wireless Traffic*  
185 *Measurements and Modeling: June 5, 2016, Seattle, WA, USA*. Berkeley, CA:  
186 USENIX Association. Retrieved from <http://portal.acm.org/toc.cfm?id=1072430>

Table 1

*Patient Characteristics*

<b>**Characteristic**</b>	<b>**In Situ**</b> , N = 127	<b>**Y-graft**</b> , N = 165	<b>**p-value**</b>
Patient Age	61 (8)	62 (8)	0.8
BMI	27.1 (4.1)	27.0 (5.0)	0.8
Hypertension	81 / 127 (64%)	100 / 165 (61%)	0.6
Hypercholesterolemia	73 / 127 (57%)	95 / 165 (58%)	>0.9
Diabetes	24 / 127 (19%)	40 / 165 (24%)	0.3
Diabetes on Insulin	1 / 127 (0.8%)	4 / 165 (2.4%)	0.3
Sex			0.7
Female	8 / 127 (6.3%)	12 / 165 (7.3%)	
Male	119 / 127 (94%)	153 / 165 (93%)	
Preoperative Creatinine	0.93 (0.21)	0.95 (0.52)	0.7
ON Pump	112 / 127 (88%)	140 / 165 (85%)	0.4
CPB Time	101 (29)	100 (34)	>0.9
XC Time	70 (22)	70 (25)	0.9

Table 2

*True and Predicted Configuration*

<b>**Characteristic**</b>	<b>**In Situ**</b> , N = 127	<b>**Y-graft**</b> , N = 165	<b>**p-value**</b>
Predicted			<0.001
In Situ	122 / 127 (96%)	8 / 165 (4.8%)	
Y-graft	5 / 127 (3.9%)	157 / 165 (95%)	
Sex			0.7
Female	8 / 127 (6.3%)	12 / 165 (7.3%)	
Male	119 / 127 (94%)	153 / 165 (93%)	

Table 3

*Graft Configuration vs. Anatomical Vessel Distribution*

<b>**Characteristic**</b>	<b>**In Situ**</b> , N = 127	<b>**Y-graft**</b> , N = 165	<b>**p-value**</b>
Left Anterior Descending	126 / 127 (99%)	165 / 165 (100%)	0.3
Intermedial Branch	47 / 127 (37%)	32 / 165 (19%)	<0.001
First Marginal	46 / 127 (36%)	31 / 165 (19%)	<0.001
Second Marginal	7 / 127 (5.5%)	1 / 165 (0.6%)	0.011
Sex			0.7
Female	8 / 127 (6.3%)	12 / 165 (7.3%)	
Male	119 / 127 (94%)	153 / 165 (93%)	

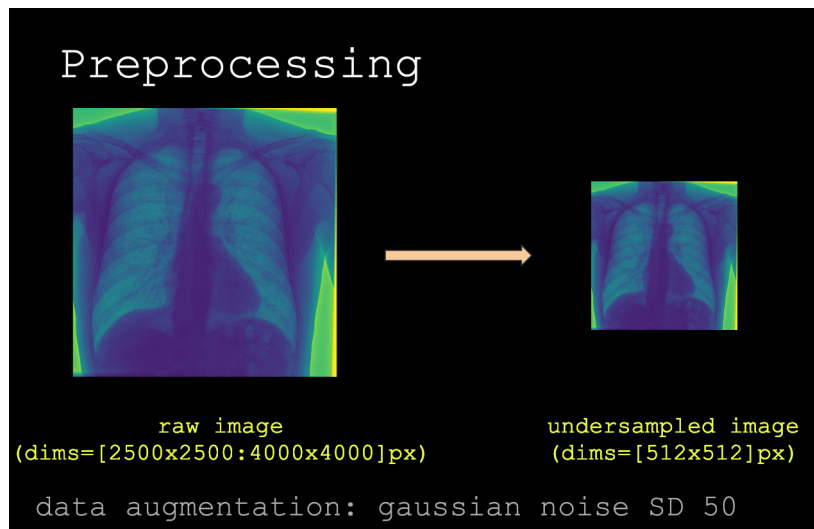


Figure 1. Figure preprocessing before feeding into neural networks.

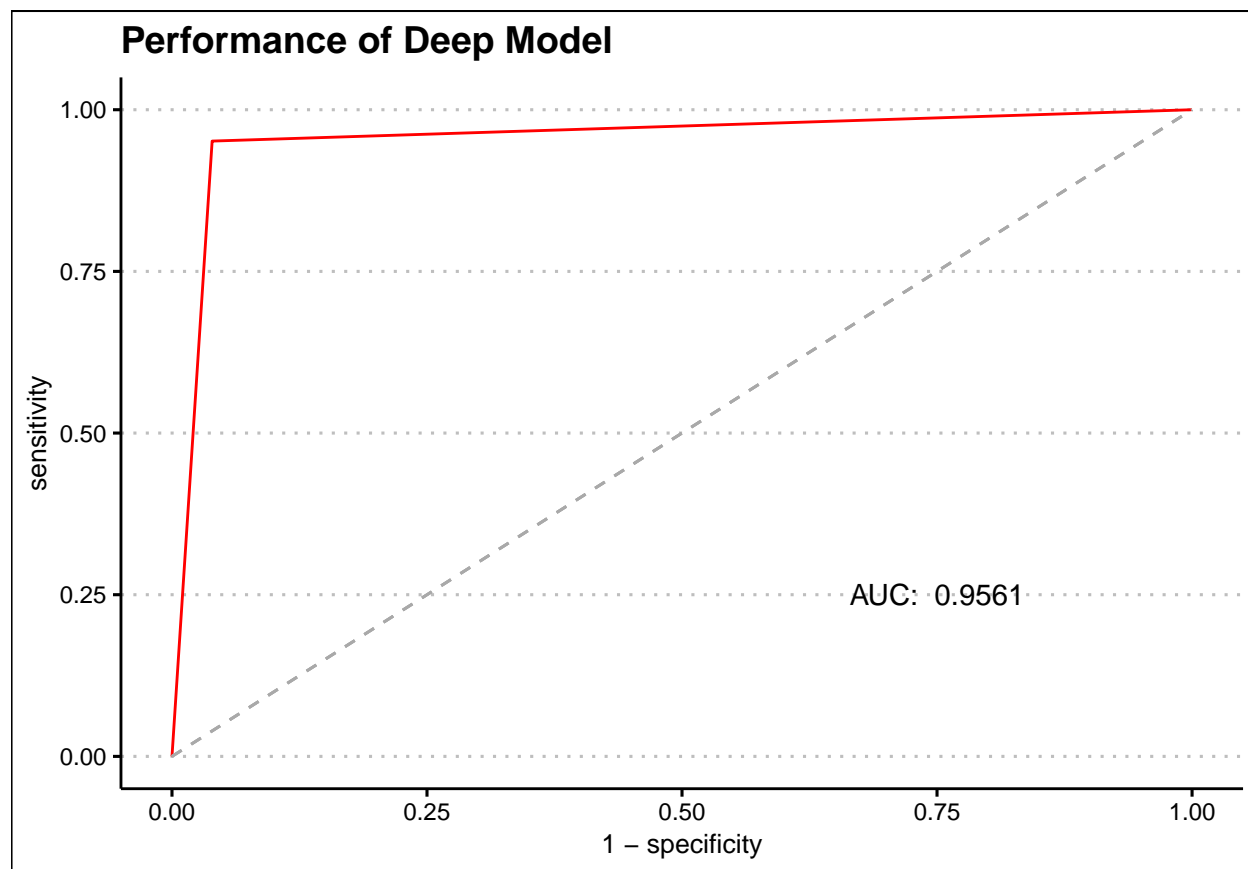


Figure 2. Model performance expressed with ROC (receiver operating characteristic) curve.